Biochimica et Biophysica Acta, 773 (1984) 219–230
Elsevier

BBA 72069

ROLE OF MEMBRANE PROTEINS AND LIPIDS IN WATER DIFFUSION ACROSS RED CELL MEMBRANES

JAMES A. DIX * and A.K. SOLOMON

Biophysical Laboratory, Department of Physiology and Biophysics, Harvard Medical School, Boston, MA 02115 (U.S.A.)

(Received September 26th, 1983)

Key words: Water diffusion; Membrane protein; Membrane lipid; Halothane quenching; N-Phenyl-1-naphthylamine; Fluorescence; NMR; (Erythrocyte)

When human red cells are treated with the mercurial sulfhydryl reagent, *p*-chloromercuribenzene sulfonate, osmotic water permeability is suppressed and only diffusional water permeability remains (Macey, R.I. and Farmer, R.E.L. (1970) Biochim. Biophys. Acta 211, 104–106). It has been suggested that the route for the remaining water permeation is by diffusion through the membrane lipids. However, after making allowance for the relative lipid area of the membrane, the water diffusion coefficient through lipid bilayers which contain cholesterol is too small by a factor of two or more. We have measured the permeability coefficient of normal human red cells by proton T_1 NMR and obtained a value of $4.0 \cdot 10^{-3}$ cm $\cdot$ s^{-1}, in good agreement with published values. In order to study permeation through red cell lipids we have perturbed extracted red cell lipids with the lipophilic anesthetic, halothane, and found that halothane increases water permeability. The same concentration of halothane has no effect on the water permeability of human red cells, after maximal pCMBS inhibition. In order to compare halothane mobility in extracted red cell membrane lipids with that in red cell ghost membranes, we have studied halothane quenching of *N*-phenyl-1-naphthylamine by equilibrium fluorescence and fluorescence lifetime methods. Since halothane mobility is similar in these two preparations, we have concluded that the primary route of water diffusion in pCMBS-treated red cells is not through membrane lipids, but rather through a membrane protein channel.

Introduction

A primary route for water entrance into the human red cell is passage through an aqueous channel [1]. Macey et al. [2] have suggested that passage through the lipid bilayer provides an additional important pathway for water diffusion into the human red cell. When water crosses lipid bilayers by diffusion, the diffusional permeability coefficient, P_d, is equal to the permeability coefficient when the driving force is osmotic pressure, P_f. The equality of these coefficients, which was established for lipid bilayers by Cass and Finkelstein [3], is widely accepted as evidence that water permeates the lipid bilayer by a diffusional process. Macey et al. [2] compared P_d for red cell membranes that had been treated with the mercurial water transport inhibitor, pCMBS, (*p*-chloromercuribenzene sulfonate) with P_f and found them to be virtually equal. Under these conditions, the diffusional permeability coefficient has dropped to 46% of that in the untreated cell [2,4,5]. Macey et al. [2] attributed this remaining portion of red cell water permeation to diffusion through the red cell lipids because the diffusional permea-

* Present address: Department of Chemistry, SUNY Binghamton, Binghamton, NY 13901, U.S.A.

Abbreviations: pCMBS, *p*-chloromercuribenzene sulfonate; Hepes, 4-(2-hydroxyethyl)-1-piperazineethanesulfonic acid.

bility of the pCMBS-treated red cell appeared to be similar to the diffusional permeability of water through phosphatidylcholine bilayers. We have made a more accurate computation which takes account of the fact that only 43% of the red cell membrane area is lipid [6] and shows that the lipid diffusional permeability coefficient, $P_{d,\,lipid}$ would have to be $5.3 \cdot 10^{-3}$ cm $\cdot$ s^{-1} to account for the diffusion Macey et al. attributed to the lipid. Cholesterol, which is present in the red cell membrane at a concentration of 0.8 mol cholesterol/mol phospholipid [6], reduces the water permeability of phosphatidylcholine bilayers. Finkelstein [7] gives $0.57 \cdot 10^{-3}$ cm $\cdot$ s^{-1} as the permeability coefficient for cholesterol/phosphatidylcholine bilayers at 25°C; Fettiplace's [8] permeability coefficients decrease from $3.7 \cdot 10^{-3}$ cm $\cdot$ s^{-1} for pure phosphatidylcholine bilayers to $1.4 \cdot 10^{-3}$ cm $\cdot$ s^{-1} at maximal cholesterol. Taking these factors into consideration, the diffusional permeability coefficient of a cholesterol/phosphatidylcholine bilayer becomes too small by a factor of two to ten to account for the apparent diffusion of water through the lipid moiety of the human red cell.

In view of this discrepancy, we have compared water diffusion through pCMBS-treated red cells with that through extracted red cell lipids, using a perturbation method. We have found that the lipophilic anesthetic, halothane (2-bromo-2-chloro-1,1,1-trifluoroethane), increases the permeability of liposomes made from red cell membrane lipids to water. We then used proton nuclear magnetic resonance to study the effect of the same halothane concentration on water diffusion in intact red cells after blocking the aqueous pores with pCMBS. We found that halothane had virtually no effect on water permeability of the intact whole cell. Control experiments showed the halothane concentration and mobility in the liposomes to be essentially the same as that in situ in the red cell membrane lipids.

Materials and Methods

NMR measurements. Fresh blood, obtained by venipuncture from healthy adults, was collected into heparinized flasks (20 units/ml blood) and used within 12 h. The cells were centrifuged and the plasma and buffy coat removed. The cells were then washed three times in NMR buffer (153 mM NaCl/5 mM KCl/5 mM Hepes (pH 7.4, 290 mosM)). For experiments with pCMBS, 0.5 ml of packed cells were incubated with 1.5 ml of 2 mM pCMBS in NMR buffer for 25 min at 26–28°C. In experiments without pCMBS, cells were treated in the same way except for pCMBS addition. At the end of the incubation, 0.5 ml of 113 mM $MnCl_2$ (290 mosM) was added to the sample to give a final hematocrit of 0.18–0.20. The sample was shaken gently and then immediately transferred to an NMR tube for measurement of proton T_1. The time from the addition of $MnCl_2$ to the end of the T_1 measurement was typically 2 min. Halothane was added as a saturated buffer solution whose concentration was assumed to be 40 mM.

The depletion of halothane from buffer was measured by ^{19}F-NMR. Packed aliquots of fresh, washed cells were suspended to 0.20 hematocrit in NMR buffer containing 20 mM halothane. The cell suspension was then centrifuged and the supernatant collected. The intensity of the halothane ^{19}F signal of the supernatant was measured by integration of the Fourier transform of the free induction decay. Typically, ten measurements were made for each sample, alternating with a measurement of the intensity of a standard solution containing 20 mM halothane. The intensity of the supernatant signal, relative to the standard, was compared with the intensity, relative to the same standard, of the signal from a 20 mM halothane solution, containing an additional 20% of NMR buffer.

Proton magnetization was measured with a JEOL FX-60 spectrometer operating at 60 MHz. A concentric capillary filled with 99.996% ^2H_2O provided an external field-frequency lock. All measurements were done at the ambient probe temperature of 26–28°C. Triplicate or quadruplicate samples were prepared and measured. Sample tubes of 10 mm diameter were used.

The spin-lattice relaxation time, T_1, was measured by the inversion-recovery method. Sufficient signal to noise ratios were obtained with a single pulse sequence. Values of the delay time between the 180° and 90° pulses ranged from 15 ms to 50–100 ms. The free induction decay was transferred to a PDP 11/34 computer by an interface described previously [9]. This rapid transfer of

data from spectrometer to computer enabled 21 free induction decays to be sampled in 90 s.

The free induction decay for each delay time was Fourier transformed and integrated, yielding a value for the total magnetization. The relaxation time-course includes contributions from three spin systems as shown in Fig. 6 and described in the appendix. The proton exchange between cell water and extracellular water is described by a single exponential process, whose rate constant can be obtained from the observed data by the method described in the appendix. Since the exchange term dominates the middle exponential, the time-course for the middle exponential, as shown in Fig. 1, is obtained by non-linear least squares. The intracellular-to-extracellular exchange time for water is then extracted from the fitted exponential time constant as described in the appendix.

Fluorescence measurements. Human red cell ghost membranes were prepared from either fresh blood or outdated bank blood. Cells were washed twice in 160 mM NaCl, then hemolyzed in 20 vol. of 5 mM sodium phosphate buffer (pH 8). The membranes were washed four times in the phosphate buffer and resuspended in NMR buffer. Red cell lipids were extracted from ghost membranes made from fresh human blood using chloroform/methanol/water by the method of Jennings and Solomon [10]. The lipids in chloroform were rotary-evaporated and then resuspended in NMR buffer.

Ghost membranes were labeled with *N*-phenyl-1-naphthylamine by adding, with vigorous stirring, aliquots of 10 mM *N*-phenyl-1-naphthylamine in methanol to a 0.5 mg protein/ml ghost suspension; the final phenylnaphthylamine/lipid ratio, assuming that the ghost membrane is 50% lipid by weight and that the average molecular weight of lipid is 750 g/mol, was 1 : 500. Lipid extracts were labeled with *N*-phenyl-1-napththylamine by adding 10 mM *N*-phenyl-1-naphthylamine in methanol to 1 mg/ml lipid suspensions; the final phenylnaphthylamine/lipid ratio was approx. 1 : 500. Halothane was added as a saturated buffer solution.

Equilibrium fluorescence was measured in a Perkin-Elmer MFP-2A spectrometer (Norwalk, CT) at room temperature. For *N*-phenyl-1-naphthylamine, the excitation wavelength was 350 nm and the emission wavelength was 420 nm. No shift in the *N*-phenyl-1-naphthylamine emission maximum was detected when halothane was added. Nanosecond lifetime measurements were measured by the modulation technique at 6 MHz, 18 MHz and 30 MHz in a SLM 4000 (SLM Instruments, Urbana, IL) instrument. For lifetime measurements, an excitation wavelength of 342 nm was used and two Corning 3-144 filters were used to select emission wavelengths greater than 420 nm.

Osmotic shrinkage measurements. Red cell lipids in chloroform, prepared as described above, were rotary evaporated to dryness, then resuspended at 0.1–0.3 mg/ml in 40 mM NaCl, 5 mM sodium phosphate, pH 7.4. The shrink solution consisted of 500 mM NaCl, 5 mM sodium phosphate, pH 7.4. Appropriate amounts of a halothane-saturated buffer solution were added to both lipid solution and shrink solution.

The osmotic shrinkage of the liposomes was measured by the method of Bangham et al. [11] using absorbance changes at 570 nm. Equal volumes of lipid and buffer solutions were mixed by hand-driven syringes in a mixing chamber described previously (Sidel and Solomon [12]); the dead time of the apparatus was 60 ms. The analog signal from the photomultiplier which measured the time-course of shrinkage was digitized by a Biomation Model 510 waveform recorder (Cupertino, CA) and transferred to a PDP 11/34 computer (Digital Equipment Corp., Maynard, MA) for data analysis. A single exponential function was fit to the data by the non-linear least-squares method.

$^{54}Mn^{2+}$ flux measurements. Washed fresh cells were suspended at 50% hematocrit in NMR buffer containing 20 mM Mn^{2+} and 0.17 μCi/ml $^{54}Mn^{2+}$ with 2 mM pCMBS as indicated. The experiments were done at 28°C. At various times after the addition of cells to buffer, 0.5 ml aliquots of the suspension were removed. The cells were spun down in an air driven microfuge (Beckman, Palo Alto, CA) and washed three times with 1 ml of ice-cold NMR buffer. 100-μl samples of the packed cell suspension were counted in quadruplicate in a gamma counter (Nuclear-Chicago, Des Plaines, IL).

Chemicals. *N*-Phenyl-1-naphthylamine was obtained from Eastman Kodak Co. (Rochester, NY).

Halothane was obtained by gift from Dr. E. Fossel. pCMBS was obtained from Sigma Chemical Co. (St. Louis, MO). $^{54}MnCl_2$ was obtained from New England Nuclear (Boston, MA).

Results and Discussion

Measurements of water diffusion

As described in the methods section, water diffusion was measured by proton nuclear magnetic resonance spectrometry using the T_1 method [13–15]. Fig. 1 shows typical data for the decay of bulk proton magnetization at times greater than 15 ms, fitted to a single exponential function by non-linear least squares. Both the T_1 and T_2 methods require the addition of Mn^{2+} to the extracellular solution which complicates the interpretation of the data since pCMBS makes the red cell permeable to Mn^{2+} (Weed and Rothstein [16]). Fig. 2a shows the experimentally measured relative rate constant for water exchange as a function of the time after cells had been exposed to both 2 mM pCMBS and 20 mM Mn^{2+}. The diffusion rate

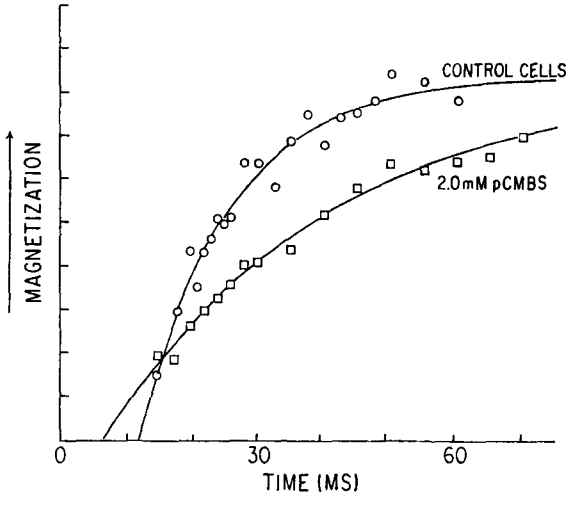

Fig. 1. Time-course of total magnetization of protons after 180° pulse; control cells (○); pCMBS-treated (2.0 mM) cells (□). There are three exponentials over the entire time-course of the relaxation of Z-magnetization. Over the limited time range shown in the figure, the data can be described by a single exponential, as discussed in the methods section. The curves have been fitted with single exponentials by the non-linear least-squares method. Since the time constants are independent of the amplitudes, we have not normalized either of the curves to a standard proton sample.

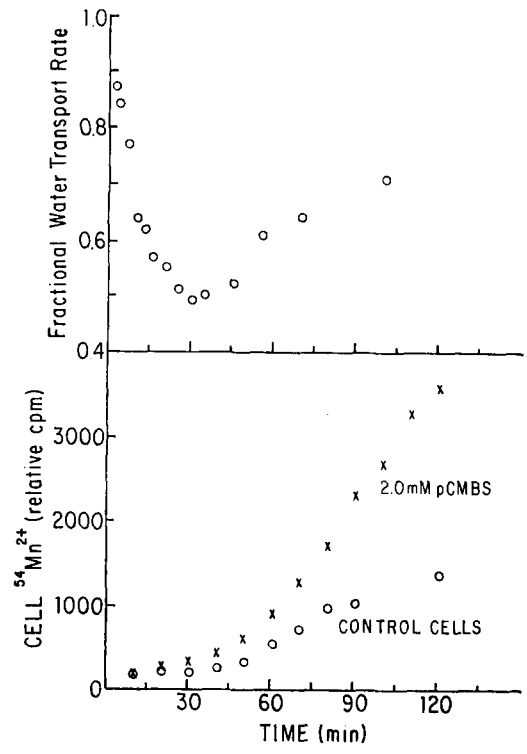

Fig. 2. (a) Time dependence of 2.0 mM pCMBS inhibition of water transport across human red cell membranes. (b) Effect of pCMBS on rate of leakage of $^{54}Mn^{2+}$ (20 mM) into intact human red cells; control (○), +2.0 mM pCMBS (×).

constant falls to a minimum of 50% of control at about 30 min after addition of the pCMBS and then rises slowly. In order to determine whether the rise can be attributed to the entrance of Mn^{2+} into the cells, we measured the uptake of Mn^{2+} into red cells with $^{54}Mn^{2+}$ following the procedure of Weed and Rothstein [16] who found that Mn^{2+} entered the red cells very slowly by passive diffusion with a permeability coefficient of $2.9 \cdot 10^{-13}$ $cm \cdot s^{-1}$. Under conditions similar to those of our NMR experiments, there is a significant increase in the intracellular concentration of Mn^{2+} at times greater than 30 min after addition of pCMBS, as shown in Fig. 2b. The measurement of the exchange rate by NMR assumes that the slow exponential decrease in magnetization is dominated by an intracellular-to-extracellular water transport. As Mn^{2+} enters the cell, there is an additional contribution to the slow exponential from the intracellular proton relaxation, caused by electron

spin-nuclear spin dipolar coupling of Mn^{2+} with intracellular water protons. The increase in the apparent rate of water transport seen in Fig. 2a for times greater than 30 min, can be accounted for by pCMBS enhanced Mn^{2+} entry into the cell. In the determination of the effect of pCMBS on water transport, therefore, cells were incubated 25–30 min before measurement, and Mn^{2+} was added just prior to the measurement. 113 mM $MnCl_2$ was used as a stock solution instead of more concentrated stock solutions used by previous investigators so that cells were not subject to osmotic shock. The dependence of the relative rate of water transport on pCMBS concentration is shown in Fig. 3. As previously found by others [4,17,18], the water flux is maximally inhibited at 2 mM pCMBS. The concentration at which the inhibition is half maximum is 0.35 mM, in reasonable agreement with the value of 0.2 mM determined by osmotic water measurements [17] and of 0.15 mM determined by interactions of pCMBS with anion transport inhibitors [1].

There have been a number of measurements of P_d, some using ^3HHO and others using proton or ^{17}O-NMR. The physical quantity measured is the

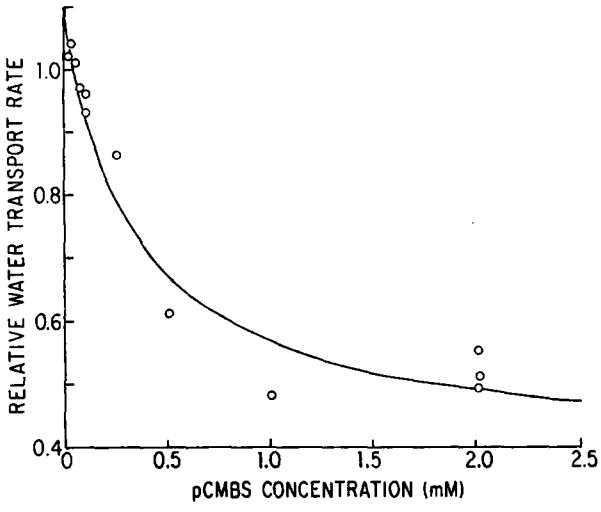

Fig. 3. Concentration dependence of pCMBS inhibition of water diffusion into intact human red cells, as measured by the T_1 method. In order to estimate the concentration for half-maximum inhibition, the line has been fitted to a single site binding model by non-linear least squares. As can be seen by inspection of the data, the half-maximum is essentially independent of the model chosen. The errors were typically 10–15%.

rate, k, of water diffusion across the cellular membrane, a parameter with dimensions of s^{-1}. The radioactivity measurements depend on the rate at which tracer-labeled water crosses the membrane; the NMR methods depend upon the rate of diffusion of proton or ^{17}O magnetization. The results have frequently been given in terms of the diffusional coefficient, P_d in $cm \cdot s^{-1}$, which is computed from k using the area, A, and volume, V, of the red cell ($P_d = k(V/A)$). Different authors have used different values of V and A and measurements have been made at different temperatures. In order to compare our results with previous ones we have converted them all to the parameter T_e ($= k^{-1}$) and to the same temperature, 20°C, as given in Table I. In order to avoid any assumptions about cell dimensions, we have based our calculations on the actual rate constants measured by the investigators, and have adjusted this figure to 20°C using the activation energy of 5.3 kcal · mol^{-1} given by Fabry and Eisenstadt [14], which agrees with the value of 6.0 kcal · mol^{-1} given by Vieira et al. [21] and that of 5.0 kcal · mol^{-1} given by Brahm [27].

The diffusional permeability coefficients reported in Table I fall into two classes: those centered around $4.2 \cdot 10^{-3}$ $cm \cdot s^{-1}$ (the first ten values, average $(4.2 \pm 0.5) \cdot 10^{-3}$ $cm \cdot s^{-1}$) and those centered around $2.4 \cdot 10^{-3}$ $cm \cdot s^{-1}$ (the last five values, average $(2.4 \pm 0.2) \cdot 10^{-3}$ $cm \cdot s^{-1}$). The reason for the apparent discrepancy in measured permeability coefficients is not known, but there are at least two complications arising from measurement of water exchange rates by NMR. The first complication occurs when exchange is measured by water proton T_1 methods. With this method, the decay of bulk magnetization is triphasic because of spin diffusion between intracellular water protons and hemoglobin protons. Neglect of spin diffusion leads to an overestimate of the exchange time (Fabry and Eisenstadt [14]). The exchange rates reported by Brooks et al. [28] and the exchange rate calculated from the T_1 measurements of Chien and Macey [24] were not corrected for spin diffusion.

The second complication occurs when water exchange is measured in red cells suspended in plasma. As Conlon and Outhred [4] have pointed out, red cells form rouleaux in albumin-containing

TABLE I

DIFFUSIONAL PERMEABILITY OF THE HUMAN RED CELL

In the section on 'Data as reported' the number of experiments, given in parentheses, is placed in the column under the parameter that was actually reported. When there are no parentheses, the number of experiments was not recorded. Conversions to the standard temperature of 20°C were made using the activation energy of 5.3 kcal·mol^{-1} given by Fabry and Eisenstadt [14]. The value of P_d in the last column was calculated from T_e using a V/A ratio of $5.33 \cdot 10^{-5}$ cm ($V = 100 \cdot 10^{-12}$ cm^3; $A = 1.35 \cdot 10^{-6}$ cm^2; cell H_2O content = 0.72). The ^{3}HHO coefficients were increased by 14% to take account of the difference in the bulk water diffusion coefficient between ^{3}HHO and H_2O [19,29] except for the data of Brahm who did not consider this correction warranted in his experiments. We have omitted from this table the water exchange rate reported in the 1975 paper of Fabry and Eisenstadt [13] (T_1 method; $T_e = 21.7 \pm 2.5$ at 25°C). This value was subsequently shown by these authors to be in error due to neglect of spin diffusion [14]. In these studies red cells were suspended in an albumin-containing medium with low Mn^{2+} concentration. As pointed out by Conlon and Outhred [4], red cells form rouleaux in albumin containing media and rouleaux formation is reversed at high Mn^{2+} concentrations. Rouleaux formation would provide a larger effective cell volume, thus increasing the measured exchange time. The flow-tube experiments of Brahm [27] have shown that high concentrations of Mn^{2+} do not affect water exchange rates.

	Data as reported				Corrected to 20°C, H_2O, standard cell	
	k (s^{-1})	T_e (ms)	Temp. (°C)	Method	t_e (ms)	P ($cm \cdot s^{-1}$)($\times 10^3$)
Paganelli and Solomon (Barton) [a] [19]	87 ±24 (7)	11.5	23	^{3}HHO	12.6	4.2
Barton and Brown [20]	91 ±22(10)	10.9	23	^{3}HHO	11.9	4.5
Vieira et al. [21]	76 ±26	13.1	22	^{3}HHO	13.9	3.8
Osberghaus et al. [22] [b]	69.4	14.4	20	^{3}HHO	14.4	3.7±0.1
Conlon and Outhred [23,4]	91.9	11.0±0.4 (9)	25	T_2	12.8	4.2
	82	12.2±1 (12)	20	T_2	12.2	4.0
Chien and Macey [24]	90.9	11.0±0.6 (9)	25	T_2	12.8	4.2
Morariu and Benga [25]	167	6.0±0.5(38)	37	T_2	9.9	5.4
Fabry and Eisenstadt [14]	82	12.2±0.9	25	T_1, T_2, T_{12}	14.2	3.8
This paper	92	10.9±1.8 (7)	27	T_1	13.4	4.0
Values that diverge from the mean above						
Brahm [27]	52.6± 4.4 (18)	19.0	25	^{3}HHO	22.1	2.4
Shporer and Civan [26]	60	16.7	25	^{17}O T_1	19.4	2.7
Pirkle et al. [15]	47.6(10)	21.0±0.6	23	T_2	23.0	2.3
Brooks et al. [28]	53	19	25	T_1	22.1	2.4
Chien and Macey [24]	58.1	17.2±0.1 (5)	25	T_1	20.0	2.6

[a] As originally pointed out by Villegas et al. [30] there was an error in the original Paganelli and Solomon [19] paper that arose from including a calculated zero-time point. Subsequently Barton and Brown [20] repeated the Paganelli and Solomon experiment using the original apparatus and corrected this error; their corrected value is used in Table I.

[b] Osberghaus et al. [22] measured ^{3}HHO diffusion through packed erythrocytes in capillary tubes. The measured quantity in this study was the rate of disappearance of ^{3}HHO from the tubes, from which a permeability coefficient was calculated. We have included in the table their permeability coefficient and back calculated the equivalent exchange time.

media and rouleaux formation is reversed at high Mn^{2+} concentrations. Rouleaux formation would provide a larger effective cell volume, thus leading to an overestimate in the exchange time. The study of Brooks et al. [28] used cells suspended in plasma, and the study of Pirkle et al. [15] used cells suspended in plasma with a low concentration of Mn^{2+}. High concentrations of Mn^{2+} do not affect water exchange rates [27]. We conclude that the diffusional permeability of Pirkle et al. [15], Brooks et al. [28] and that calculated from the T_1 studies of Chien and Macey [24] are probably underestimates due to neglect of spin diffusion and rouleaux formation.

The best estimate of the diffusional permeability of water in red cells is probably the average of the first ten values in Table I: $(4.22 \pm 0.49) \cdot 10^{-3}$ $cm \cdot s^{-1}$. This value includes measurements by ^{3}HHO exchange by two different methods [19–22]; and measurements by proton T_1 (Ref. 14 and this

paper), T_2 [4,14,23–25] and hybrid T_1/T_2 [14] NMR methods. The reasons that the values reported by Shporer and Civan [26] and Brahm [27] lie outside this range are not known, although the ^{17}O-NMR measurements of Shporer and Civan [26] are subject to large errors because the intrinsic decay of water ^{17}O is similar to the exchange times.

Perturbation of water diffusion by halothane

The rationale of these experiments was to use a lipophilic solute to perturb the lipid bilayer. Comparison of halothane effects on the water permeability of the intact red cell membrane and on that of a total lipid extract would reveal similarities and differences between the two systems. Intact red cells that had been maximally inhibited with pCMBS were used to examine the effect of halothane on red cell water flux. If pCMBS completely inhibits protein-mediated water transport, the remaining water flux should be through the lipids and therefore should be sensitive to halothane. The first two columns of Table II show that halothane has no effect on the relative water permeability of pCMBS (2.0 mM)-treated intact red cells. The relative rate in pCMBS-treated red cells was obtained by dividing the observed rate (with halothane) by the rate in the absence of halothane. The relative rate was independent of halothane concentration and averaged 0.96 ± 0.10, not significantly different from unity. Thus halothane had no perceptible effect on the permeability of pCMBS-treated intact cells. Similar results were obtained with cells not treated with pCMBS (data not shown).

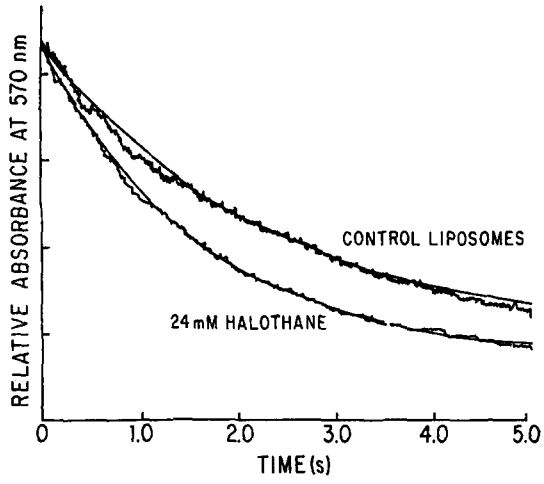

Fig. 4. Relative time-course of shrinkage of liposomes made from extracted red cell lipids. The time constant for the control is 2.3 ± 0.2 s and for the halothane treated liposomes, 1.6 ± 0.2 s. The curves have been fitted with single exponentials by non-linear least squares.

To determine whether these concentrations of halothane perturb red cell lipids sufficiently to affect water transport, we extracted the red cell lipids from the membrane and measured the water flux through the extracted lipids as a function of halothane concentration. In these measurements, the rate of water transport was taken to be proportional to the exponential rate constant of liposome shrinkage determined by absorbance changes at 570 nM. Typical data and fitted exponential curves are shown in Fig. 4.

TABLE II

EFFECT OF HALOTHANE ON WATER PERMEABILITY

pCMBS concentration was 2.0 mM. The relative rate is obtained by dividing the rate observed in the presence of halothane by the control rate in the absence of halothane.

pCMBS-treated red cells		Extracted red cell lipids		Ratio
Halothane (mM)	Relative rate	Halothane (mM)	Relative rate	
6.2	0.96	6.1	1.16	1.21
7.1	0.81	8.0	1.16	1.43
12.0	0.99	11.0	1.32	1.33
14.3	0.97	15.0	1.34	1.38
18.0	1.11	16.0	1.26	1.14
21.4	0.92	24.0	1.27	1.38
Ave	0.96 ± 0.10		1.25 ± 0.08	1.31 ± 0.12

TABLE III

NANOSECOND FLUORESCENCE LIFETIME MEASUREMENTS

The fluorescence lifetime of phenylnaphthylamine bound to ghost membranes was measured by the phase modulation technique in a SLM lifetime instrument; two lifetimes are obtained by this technique, a modulation lifetime, τ_m, and a phase lifetime, τ_p. If $\tau_m \neq \tau_p$, then the frequency dependence of τ_m and τ_p can be analyzed in terms of two or more lifetimes. An analysis based on two lifetimes gives 8.6 ns and 2.3 ns, with fractional populations of 0.87 and 0.13, for control ghosts. For halothane ghosts, the lifetimes are 7.2 ns and 2.8 ns, with fractional populations of 0.43 and 0.57.

Measurement	Frequency	6 MHz (ns)	18 MHz (ns)	30 MHz (ns)
Control ghosts	τ_m	8.5 ± 0.5	8.2 ± 0.6	7.9 ± 0.2
	τ_p	7.6 ± 0.4	7.0 ± 1.5	6.7 ± 0.4
Ghosts + 20 mM halothane	τ_m	5.8 ± 0.8	5.1 ± 0.1	4.8 ± 0.1
	τ_p	4.6 ± 0.3	4.3 ± 0.3	3.9 ± 0.2

The relative rate of water transport through extracted red cell lipids as a function of halothane concentration is also given in Table II (columns 3 and 4). As the table shows, there is a tendency for the rate to increase with increasing halothane concentration. The average relative rate at all concentrations is 1.25 ± 0.08, significantly greater than 1.0 (t-test, $P < 0.005$). We have also formed the ratio, at paired concentration points, of the relative rate of water flux in red cell liposomes, divided by that in the intact cells, shown in the last column of Table III. The average value of this ratio is 1.31 ± 0.12 which is also significantly different from unity (t-test, $P < 0.0025$). These data show that halothane, at solution concentrations high enough to affect water transport through extracted red cell lipids, does not affect water transport in intact red cell membranes.

Membrane concentration and mobility of halothane

The most important determinants of the effect of halothane on red cell lipids are halothane concentration and mobility within the membrane. The partition coefficients of halothane have been determined by Miller and his colleagues [31,32]. Smith et al. [31] have measured the partition coefficient for halothane in human red cell ghosts at 25°C and found a value of 35 ± 5 (volume of pure solute gas corrected to 0°C and 1 atm pressure dissolved in unit volume of solvent). Using the relative protein and lipid content of human red cell ghost membranes of 49.2% and 43.6% (by weight) given by Guidotti [33] and protein and lipid densities of 1.2 and 0.95, we can compute that the partition coefficient for halothane in the lipids of ghost membranes is 72. The partition coefficient in lipid bilayers (96% phosphatidylcholine, 4% phosphatidic acid plus 33 mol% cholesterol) is given by Smith et al. [31] as 93. Furthermore, Korten et al. [32] report that partition coefficients in lipid bilayers made from lipids extracted from red cell ghosts are comparable to those in corresponding egg phosphatidylcholine/cholesterol bilayers. Thus there is relatively little difference between the halothane partition coefficients in red cell lipids in ghosts and that in lipid bilayers.

Since the lipid content of the preparations used for the osmotic swelling experiments differs from that in the NMR experiments, and since the partition coefficient is high, it is necessary to check that halothane loss from the external solution is negligible. In our extracted red cell lipid suspension the relative lipid volume is $3 \cdot 10^{-4}$ so that the halothane depletion from the supernatant would only be 3%, using a mean partition coefficient of 85. In our intact red cell suspension the hematocrit is 0.2, and the lipid is 0.95 μl/ml suspension, so that halothane depletion is 8%. These relatively small corrections do not affect the conclusions of this paper. We confirmed the intact membrane calculation by measuring the halothane concentration in buffer by ^{19}F-NMR. The ratio of buffer halothane concentration in the presence of red cells to that without cells was 0.94 ± 0.10 (S.E., $n = 5$), not appreciably different from 1.

An alternative explanation for the absence of halothane effect on intact red cell water transport is that halothane, while associated with the cell membrane, may not be associated with the red cell lipids. To study mobility of halothane in red cell lipids, the lipids were labeled with the fluorescent probe *N*-phenyl-1-naphthylamine, which fluoresces strongly when bound to lipid [34]. The phenylnaphthylamine fluorescence is quenched by halothane since chlorinated hydrocarbons are known to quench fluorescence [35]. The fluorescence quenching of phenylnaphthylamine by halothane is plotted in the form of a Stern-Volmer plot in Fig. 5. The modified Stern-Volmer equation [36] is given by

$$F_0/F = (1 + k_{sv}K[\mathrm{H}]_{tot})/e^{-k'K[\mathrm{H}]_{tot}} \quad (1)$$

in which k_{sv} is the Stern-Volmer quenching constant, K is the halothane partition coefficient, $[\mathrm{H}]_{tot}$ is the solution concentration of halothane and k' is the fractional volume of a hypothetical sphere around the fluorophore that would be occupied by a 1 M solution of quencher; static quenching is assumed to occur only if the quencher is within this hypothetical sphere. $k_{sv} = k_q \cdot \tau$ in which k_q is the bimolecular rate constant for quenching and τ is the fluorescence lifetime. In the range in which the dependence of F_0/F upon $[\mathrm{H}]_{tot}$ is linear, Eqn. 1 may be approximated by

$$(F_0/F) - 1 = k_{sv}K[\mathrm{H}]_{tot} \quad (2)$$

There are two observations to be made about the Stern-Volmer plot shown in Fig. 5. First, there is no difference between the points for extracted red cell lipids and ghost membranes and second, the data are linear up to about 20 mM halothane, almost the highest concentration used in the experiments in Table II. Linear Stern-Volmer plots are characteristic of quenching by a diffusional mechanism. The similarity of the concentration dependence of quenching for liposomes and red cell ghosts means that the product $k_{sv}K$ is the same in both systems and the linearity shows that the product is concentration-independent up to 15 mM. Since Smith et al. [31] have shown that the partition coefficient is similar in both systems, these measurements suggest that there is very little difference between k_{sv} for extracted red cell lipids and k_{sv} for intact red cell ghost membranes over the concentration range we have studied. Thus the data in Fig. 5 indicate that the halothane environment in these two systems is similar.

The upward curvature seen in the Stern-Volmer plot at high halothane concentrations is characteristic of an additional, static component to the quenching mechanism [34] which is given by the exponential term in Eqn. 1. The similarity of quenching magnitudes in red cell liposomes and in intact membranes at high halothane concentrations implies that the local, time-independent halothane concentration as seen by phenylnaph-

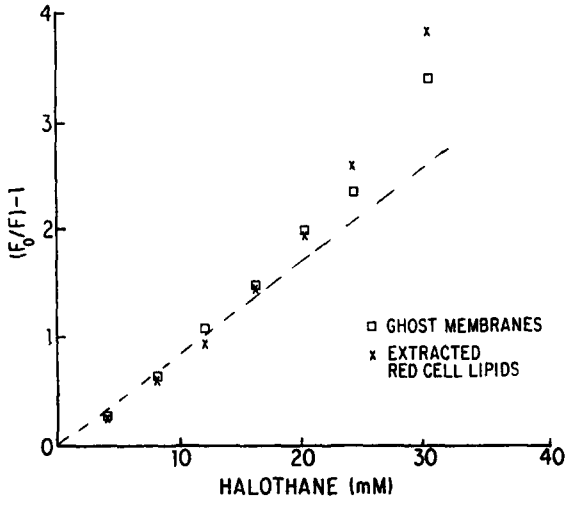

Fig. 5. Stern-Volmer plot of relative fluorescence (F_0/F) as a function of halothane concentration in the external solution; red cell ghost membranes (□); extracted red cell lipids (×).

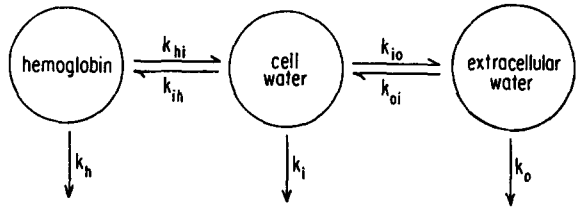

Fig. 6. Schematic representation of the three exchanging spin systems in T_1 measurements of red cell suspensions. k_h, k_i and k_o represent the rates of decay of bulk proton magnetization of hemoglobin, intracellular water and extracellular water, respectively. k_{hi} and k_{ih} are spin diffusion rates; k_{io} and k_{oi} are intracellular/extracellular exchange rates.

TABLE IV

PARAMETERS USED IN SIMULATION

Symbol	Value	Source
k_i	1.4 s^{-1}	measurement of T_1 of pellet following centrifugation of sample after experiment
k_o	133 s^{-1}	measurement of T_1 of supernatant following centrifugation of sample after experiment
k_h	0.9 s^{-1}	estimated from Eisenstadt and Fabry [43]; corrected to 60 MHz, assuming $\omega^2\tau_c^2 \gg 1$
k_{io}	varied	
k_{oi}	varied	calculated from detailed balancing; $k_{oi} = k_{io}$ (0.72 hct)/(1 − hct) where hct is the measured hematocrit and the fractional intracellular water volume is 0.72
k_{hi}	50 s^{-1}	estimated from Eisenstadt and Fabry [43]; corrected to 60 MHz, assuming $\omega^2\tau_c^2 \gg 1$
k_{ih}	19 s^{-1}	calculated from detailed balancing; $k_{ih} = 0.28k_{hi}/0.72$, assuming a fractional hemoglobin proton volume in the cell of 0.28 and that hemoglobin proton density equals water proton density

Initial conditions (hematocrit = 0.18)

Spin system	Fraction of total protons
Extracellular protons	0.82
Intracellular protons	0.13
Hemoglobin protons	0.05

thylamine in these two systems is similar. This observation supports the conclusions derived above from consideration of diffusional quenching. Taken together, these results show that halothane is able to penetrate the lipid region of these two membrane preparations, and that the absence of any halothane effect on water transport in red cells is not due to inability of halothane to partition into intact red cell lipids.

In order to investigate further the mechanism of quenching, we measured the fluorescence lifetime of phenylnaphthylamine in ghost membranes when halothane was added. The results are given in Table III. The decay of fluorescence of phenylnaphthylamine is generally complicated due to excited-state reactions [34]. Table III shows that the average fluorescence lifetime of phenylnaphthylamine decreases from 7.8 ns to 4.7 ns when halothane is added. Decreases in average fluorescence lifetimes strongly suggest that the quenching mechanism is in part due to diffusional mechanisms. Addition of 20 mM halothane decreases the average fluorescence lifetime to 60% of control, less quenching than the 33% ratio of F_0/F given in Fig. 5. This is consistent with the presence of the static component of quenching that has already been discussed. These lifetime measurements add further support to the conclusion that phenylnaphthylamine and halothane experience similar mobility in extracted red cell lipid and red cell ghost membranes.

The data presented in Table II show that halothane has no effect on the permeability of water through intact red cells that have been maximally inhibited by pCMBS, whereas halothane causes an increase in the permeability of liposomes made from a total extract of red cell lipids. There are three possible explanations for this finding: (1) the halothane mobility in the liposomes is significantly different from that in the red cell mem-

brane; (2) incorporation of red cell lipids into a red cell membrane somehow alters the lipid diffusional barrier; or (3) water permeation is associated with the red cell membrane proteins.

The partition coefficients reported by Miller and his colleagues [31,32] indicate that the solubility of halothane is similar in both systems. The fluorescence lifetime and fluorescence quenching experiments indicate that the diffusional properties of halothane are similar in both extracted red cell lipids and intact red cell ghosts. Since the presence of membrane proteins does not affect halothane mobility significantly, it is very unlikely that the proteins affect the diffusion of water through the lipid moiety. We conclude that the presence of proteins in the red cell membrane is responsible for the permeation of water in pCMBS inhibited red cells and that virtually all of red cell water transport is protein mediated. The inhibition by pCMBS of only 50% of diffusional water transport may mean that the water traverses the same channel in pCMBS treated cells as in normal controls and that the effect of pCMBS is to occlude the channel so that bulk flow is no longer possible, while not sealing it completely. Alternately, pCMBS may completely inhibit the major polar channel, and the remaining water transport go through other protein polar channels that are pCMBS insensitive.

Acknowledgement

We would like to express our thanks to Dr. Alan Kleinfeld for his advice and assistance in the fluorescence lifetime measurements and to Mr. Bernard Corrow for his help in the construction and maintenance of the apparatus. Supported in part by NSF grant PCM-78-22577 and NIH grants GM 15692 and HL 29488.

Appendix

The use of NMR to measure water exchange rates in red cell suspensions involves the measurement of the rate that nuclear spins of water exchange from inside the cell to outside the cell. The decay of magnetization under spin-exchange conditions is described mathematically by a set of coupled, linear differential equations [37–39]. If water exchange is measured by ^{17}O T_1 or T_2 methods, or by ^1H T_2 methods, then there are only two exchanging spin systems, intracellular and extracellular water, and consequently two coupled differential equations describe the decay. The magnetization from the two exchanging spin systems will decay with two time constants; each time constant contains contributions from the intrinsic decays of each system as well as the exchange rate [14,23].

If, however, water exchange is measured by ^1H T_1 methods, then there is a third spin system which contributes to the exchanging spin system. The third spin system is hemoglobin protons, which can exchange with intracellular water protons by a process known as spin diffusion [14,40,41]. Three coupled linear differential equations are needed to describe proton T_1 decay. The exchanging spin system is illustrated schematically in Fig. 6.

The three coupled linear differential equations can be written conveniently in matrix form:

$$\begin{pmatrix} \frac{dM_o}{dt} \\ \frac{dM_i}{dt} \\ \frac{dM_h}{dt} \end{pmatrix} = \begin{pmatrix} -k_o - k_{oi} & k_{io} & 0 \\ k_{oi} & -k_i - k_{io} - k_{ih} & k_{hi} \\ 0 & k_{ih} & -k_h - k_{hi} \end{pmatrix} \begin{pmatrix} M_o \\ M_i \\ M_h \end{pmatrix}$$

or

$$(A) = (B)(C)$$

The solutions for M_o, M_i and M_h are easily obtained by the Laplace transform [42]. The total magnetization decay will be the sum of three decays whose rate constants are given by the eigenvalues of the matrix B. The eigenvalues, λ, of the matrix B are the roots of the cubic equation

$$\lambda^3 + \lambda^2(-b_{11} - b_{22} - b_{33}) + \lambda(b_{11}b_{22} + b_{22}b_{33} + b_{33}b_{11} - b_{12}b_{21} - b_{23}b_{32}) - b_{11}b_{22}b_{33} + b_{11}b_{23}b_{32} + b_{12}b_{21}b_{33} = 0$$

where b_{ij} are the matrix elements of B.

In order to extract the exchange time from our data, we simulated the total magnetization decay

and fit a single exponential function to the simulated data over the time range that we acquired our experimental data. All parameters of the simulation, except for the intracellular to extracellular exchange rate, were known from independent measurements or from the literature. The exchange rate was varied until the exponential time constant from a fit of the simulated data matched that obtained from a fit of the experimental data. The experimental time constant was 13.9 ms; the exchange rate extracted from this measurement was 10.9 ms. The parameters used in the simulation are given in Table IV.

References

1 Solomon, A.K., Chasan, B., Dix, J.A., Lukacovic, M.F., Toon, M.R. and Verkman, A.S. (1983) Ann. N.Y. Acad. Sci. 414, 97–124
2 Macey, R.I., Karan, D.M. and Farmer, R.E.L. (1972) in Passive Permeability of Cell Membranes, Biomembranes, Vol. 3 (Kreuzer, F. and Slegers, J.F.G., eds.), pp. 331–340, Plenum Press, New York
3 Cass, A. and Finkelstein, A. (1967) J. Gen. Physiol. 50, 1765–1784
4 Conlon, T. and Outhred, R. (1978) Biochim. Biophys. Acta 511, 408–418
5 Ashley, D.L. and Goldstein, J.H. (1981) J. Membrane Biol. 61, 199–207
6 Rosenberg, S.A. and Guidotti, G.J. (1968) J. Biol. Chem. 243, 1985–1992
7 Finkelstein, A. (1976) J. Gen. Physiol. 68, 127–135
8 Fettiplace, R. (1978) Biochim. Biophys. Acta 513, 1–10
9 Dix, J.A. and Pandiscio, A.A. (1980) J. Magn. Resonance 39, 367–368
10 Jennings, M.L. and Solomon, A.K. (1976) J. Gen. Physiol. 67, 381–397
11 Bangham, A.D., De Gier, J. and Greville, G.D. (1967) Chem. Phys. Lipids 1, 225–246
12 Sidel, V.W. and Solomon, A.K. (1957) J. Gen. Physiol. 41, 243–257
13 Fabry, M.E. and Eisenstadt, M. (1975) Biophys. J. 15, 1101–1110
14 Fabry, M.E. and Eisenstadt, M. (1978) J. Membrane Biol. 42, 375–398
15 Pirkle, J.L., Ashley, D.L. and Goldstein, J.H. (1979) Biophys. J. 25, 389–406
16 Weed, R.I. and Rothstein, A. (1960) J. Gen. Physiol. 44, 301–314
17 Macey, R.I. and Farmer, R.E.L. (1970) Biochim. Biophys. Acta 211, 104–106
18 Naccache, P. and Sha'afi, R.I. (1974) J. Cell. Physiol. 84, 449–456
19 Paganelli, C.V. and Solomon, A.K. (1957) J. Gen. Physiol. 41, 259–277
20 Barton, T.C. and Brown, D.A.J. (1964) J. Gen. Physiol. 47, 839–849
21 Vieira, F.L., Sha'afi, R.I. and Solomon, A.K. (1970) J. Gen. Physiol. 55, 451–466
22 Osberghaus, U., Schönert, H. and Deuticke, B. (1982) J. Membrane Biol. 68, 29–35
23 Conlon, T. and Outhred, R. (1972) Biochim. Biophys. Acta 288, 354–361
24 Chien, D.Y. and Macey, R.I. (1977) Biochim. Biophys. Acta 464, 45–52
25 Morariu, V.V. and Benga, G. (1977) Biochim. Biophys. Acta 469, 301–310
26 Shporer, M. and Civan, M.M. (1975) Biochim. Biophys. Acta 385, 81–87
27 Brahm, J. (1982) J. Gen. Physiol. 79, 791–819
28 Brooks, R.A., Battocletti, J.H., Sances, A., Larson, S.J., Bowman, R.L. and Kudravcev, V. (1975) IEE Trans. Biomed. Eng. BME-22, 12–18
29 Wang, J.H., Robinson, C.V. and Edelman, I.S. (1953) J. Am. Chem. Soc. 75, 466–470
30 Villegas, R., Barton, T.C. and Solomon, A.K. (1958) J. Gen. Physiol. 42, 355–369
31 Smith, R.A., Porter, E.G. and Miller, K.W. (1981) Biochim. Biophys. Acta 645, 327–338
32 Korten, K., Sommer, T.J. and Miller, K.W. (1980) Biochim. Biophys. Acta 599, 271–279
33 Guidotti, G. (1972) Arch. Intern. Med. 129, 194–201
34 Matayoshi, E.D. and Kleinfeld, A.M. (1981) Biochim. Biophys. Acta 644, 233–243
35 Lakowicz, J.R. and Hogan, D. (1977) in Membrane Toxicity (Miller, M.W., and Shamoo, A.E., eds.), pp. 509–546, Plenum Press, New York
36 Badley, R.A. (1976) in Modern Fluorescence Spectroscopy, Vol. 2 (Wehry, E.L., ed.), pp. 112–119, Plenum Press, New York
37 McConnell, H.M. (1958) J. Chem. Phys. 28, 430–431
38 Woessner, D.E. (1961) J. Chem. Phys. 35, 41–48
39 Johnson, C.S. Jr. (1965) Adv. Magn. Resonance 1, 33–102
40 Solomon, I. (1955) Phys. Rev. 99, 559–565
41 Edzes, H.T. and Samulski, E.T. (1977) Nature 265, 521–523
42 Tamura, K. and Schelly, Z.A. (1980) J. Phys. Chem. 84, 2996–2998
43 Eisenstadt, M. and Fabry, M.E. (1978) J. Magn. Resonance 29, 591–597